Nanofluidic tuning of photonic crystal circuits

David Erickson, Troy Rockwood, Teresa Emery, Axel Scherer, Demetri Psaltis

David Erickson, Troy Rockwood, Teresa Emery, Axel Scherer, Demetri Psaltis, "Nanofluidic tuning of photonic crystal circuits," Proc. SPIE 6475, Integrated Optics: Devices, Materials, and Technologies XI, 647513 (9 February 2007); doi: 10.1117/12.711490

SPIE.

Event: Integrated Optoelectronic Devices 2007, 2007, San Jose, California, United States

Nanofluidic tuning of photonic crystal circuits

David Erickson[a], Troy Rockwood[b], Teresa Emery[b], Axel Scherer[b], and Demetri Psaltis[b]
[a]Sibley School of Mechanical and Aerospace Engineering, Cornell University, Ithaca, NY 14853.
[b]Center for Optofluidic Integration, California Institute of Technology, Pasadena, California 91125

ABSTRACT

By integrating soft-lithography-based nanofluidics with silicon nanophotonics, we demonstrate dynamic, liquid-based addressing and high $\Delta n/n$ (~0.1) refractive index modulation of individual features within photonic structures at subwavelength length scales. We show ultracompact tunable spectral filtering through nanofluidic targeting of a single row of holes within a planar photonic crystal. We accomplished this with an optofluidic integration architecture comprising a nanophotonic layer, a nanofluidic delivery structure, and a microfluidic control engine. Variants of this technique could enable dynamic reconfiguration of photonic circuits, selective introduction of optical nonlinearities, or delivery of single molecules into resonant cavities for biodetection.

Keywords: nanophotonic, photonic crystal, microfluidic, subwavelength, optofluidic

1. INTRODUCTION:

Optical devices that incorporate liquids as a fundamental part of their structure can be traced at least as far back as the 18th century, when rotating pools of mercury were proposed as a simple technique to create smooth spherical mirrors for use in reflecting telescopes.[1] Modern microfluidics has enabled the development of a present-day equivalent of such devices centered on the marriage of fluidics and optics[2–6] that we refer to as 'optofluidics.' Such devices have substantial advantages for creating adaptive optical elements including high $\Delta n/n$, inherently smooth optical interfaces, and thermal stabilization.

At present, techniques for local refractive index modulation in photonic structures are limited to the exploitation of relatively weak nonlinearities,[7] where $\Delta n/n$ is of the order of 10^{-3} or lower, and thus require long interaction lengths, high operational power, or the incorporation of resonant elements to enhance the effect. Techniques such as mechanical deformation, thermo-optics, liquid crystal infusion, and liquid fluid infusion, offer much higher effective $\Delta n/n$; however, they tend to be nonlocalized effects requiring or resulting in modification over a large area, if not the entire device. Thus whereas local tunability over small interaction lengths requires the high $\Delta n/n$ afforded by these global approaches, the ability to perform such manipulations with the submicrometer scale precision required for advanced photonic devices remains elusive. The development of such a technique could enable the creation of a new class of ultracompact adaptable photonic circuits and sensors.

Nanofluidics provides a solution that enables both localized control and high refractive index modulation. Here we demonstrate the integration of multilayer soft-lithography[8] nanofluidics with silicon nanophotonics and use it to address and tune features within planar photonic crystals.[9] Photonic crystals are attractive for controlling optical propagation by introducing pre-engineered defects into an otherwise regular lattice to create spectral filters, tight bend waveguides, resonant cavities, and highly efficient lasers. As a first step in the development of two dimensional reconfigurable photonic circuits, here we demonstrate the nanofluidic addressing of a single row of holes within a photonic crystal.

2. NANOSCALE OPTOFLUIDIC INTEGRATION:

The integration of fluidics and photonics at the 100 nanometer scale represents a significant challenge in terms of fabrication, alignment and operation. Due to the extreme difficulty in constructing a single structure which contains both the photonic and fluidic components, the general approach used here was to take advantage of standard photonic and fluidic processing (fabricating the two components separately) and then develop a technique for interfacing the two. In this section will first give a brief and general overview of micro- and nano-fabrication techniques and materials in the context of which are most suitable for integration with nanophotonic structures. We will then describe in greater detail the specifics of the fabrication procedure and general integration philosophy used here including it's advantages and

Integrated Optics: Devices, Materials, and Technologies XI, edited by Yakov Sidorin, Christoph A. Waechter,
Proc. of SPIE Vol. 6475, 647513, (2007) · 0277-786X/07/$18 · doi: 10.1117/12.711490

limitations.

2.1 Fabrication Procedure for SOI Photonic Crystals

The e-beam lithography and dry etching fabrication procedures for creating the SOI photonic crystals used are well established and well described in the literature (e.g. 12). For optofluidic integration we modify the procedure outlined in Loncar *et al.*[12] only slightly in that we defined the pattern in a negative flowable oxide resist which is left on after processing to enhance bonding with the fluidic layer. Additionally we do not etch the underside insulator layer in favor of using it to enhance the mechanical stability of the structure. In general, "flow through" photonic structures (such as membrane suspended photonic crystals) require much more complicated fluidic confinement schemes on both sides of the device and therefore well type structures are typically preferred. Figure 1 shows a sample photonic crystal used here prior to integration with the fluidics.

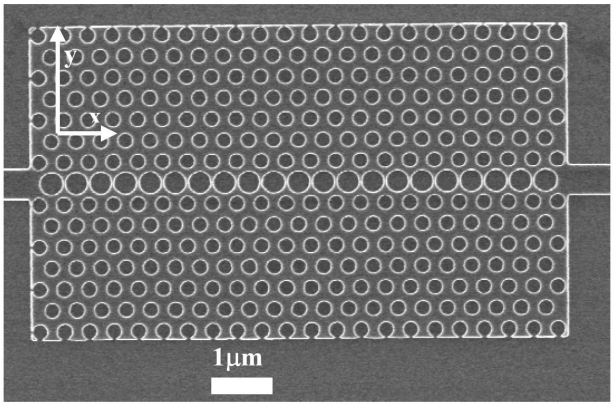

Figure 1: Silicon-on-Insulator Photonic Crystal. The lattice constant and hold radius of the crystal are 434nm and 140nm respectively and the height is 207nm out of the page. Larger holes in the center are a design-time defect done in order to introduce a guided mode into band gap of the crystal. The larger holes are those which are to be targeted fluidically.

2.2 Micro- and nano- fluidic fabrication procedures

At the onset of modern microfluidics in the early 1990's glasses, quartz and silicon were the materials of choice for microfabrication[13-16], primarily due to the well established wet etching and lithography based micromachining techniques developed by the electronics and semiconductor industries[17-18]. When defined using e-beam lithography or similar high resolution resist patterning techniques and etched using RIE or equivalent techniques resolutions on the orders required here can be obtained relatively easily. While such structures have the advantage of having a well defined, rigid geometry, optofluidic integration requires the fluidic system to travel over not only the photonic structure but also the coupling waveguides and other protruding optical structures on the base SOI substrate and thus fluidic sealing between the two rigid structures becomes difficult.

The alternative approach is to use some of the more recently developed techniques for building fluidic systems from low cost polymeric materials such as poly(dimethsiloxane) (PDMS)[19-20], poly(methylmethacrylate) (PMMA)[21-22] and others (see Becker and Locascio[23] and deMello[24] for comprehensive reviews). In general the primary attractiveness of these materials is that they tend to involve simpler and significantly less expensive manufacturing techniques (e.g. casting, injection and replica molding, or hot embossing). Of these materials and techniques, PDMS processing using the soft lithography process developed by Whitesides' group at Harvard University[20, 25, 26] is the most suitable as is electrometric nature facilitates sealing over rigid surfaces. The Quake group, then at Caltech, demonstrated how a reasonably simple two layer structure constructed using this processing can be scaled to create highly integrated devices with 1000's of valves per cm_2 (see Thorsen et al.[27] for details). This same feature also complicates the fabrication of sub-micron

channels as it deformable nature can to lead to channel collapse, though in general such problems can be avoided by manipulating the linker:base ratios and through careful processing. As a result multi-layer soft-lithography was selected as the fluidic fabrication technique for this work. In addition to manufacturing simplicity, building the fluidic layer separately from the optical layer in a soft polymer such as PDMS or RTV has the additional advantage of being air permeable which facilitates the initial wetting of the system.

2.3 Multilevel Optofluidic Integration

From an operational perspective addressing individual features within a photonic crystal necessitates the use of nanoscale fluidics, however the complex fluidic switching, dispensing and mixing required to operate such devices becomes difficult at those length scales due to the D^2 dependence of flow velocity on channel size (where D is the characteristic channel diameter) and $1/L^2$ dependence of the diffusion time (where L is the characteristic length scale for diffusion). To avoid this difficulty we developed a technique for "multilevel optofluidic integration" as described below.

The first level of integration is the nanophotonic level which comprises of the device or devices to be fluidically targeted, defined on the base substrate which also provides support for the fluidics. In this case we use an array of 30 identical photonic crystal structures defined in SOI, each with a triangular lattice of holes constant a = 434nm, hole radius r = 140nm and height h = 207nm. Ridge waveguides extend from the crystal array to the edge of the chip for optical coupling into the crystal. In the experiments presented here we increase the radius of the holes within the central row of the photonic crystal (which is to be targeted fluidically) to 203nm in order to introduce a reduced index guided mode into the band gap created by the otherwise regular crystal lattice. This geometry was selected on the basis of a series of numerical experiments as having transmission properties that were most sensitive to changes in index of refraction within the targeted region. Details on the calculations performed to reach this conclusion are outlined later.

The second level of integration for nanofluidic delivery involves defining the nanofluidic system in positive relief on a separate standard silicon substrate using processing identical to that used to define the photonic crystals. To match up with the photonic structure here we use an array of channels 200 nm tall, coinciding with the thickness of the silicon layer of the SOI material above. The 350 nm wide channels are spaced with a 5μm period.

The purpose of the nanofluidics level is to provide fluidic coupling between the photonic structure and the upper level of integration or "microfluidics engine" as described previously. To integrate the microscale fluidics we define the pattern, again in positive relief, on the same nanofluidic substrate using the following technique. After acetone and isopropyl alcohol cleaning and treating the nanofluidic substrate with an hexamethyldisilazane (HDMS) based photoresist adhesion agent, SPR 220-7 (Shipley) photo resist was spun on to a thickness of approximately 10μm. The mask containing the fluidic patterns was then aligned such that the predefined nanochannels overlapped with the microfluidic pattern to ensure efficient coupling between the two structures. The photoresist was then exposed, soft baked and developed using the procedure recommended by the manufacturer. A hard bake step at 110^0C for at least 30min was then done to harden the photoresist and enhance the adhesion. A 20-30μm thick film of 10:1 (base:linker) RTV is then spun on the master and allowed to cure for 30 minutes at 80^0C. Once the master is formed, the fluidic layer is cast in silicone elastomer.

To complete the microfluidics engine an upper control layer which contains the control valves (see Unger et al.[8] for details of valve actuation in such devices) is bonded to the fluidic system. A valve layer that provides the active control is similarly defined, cast, and bonded to the fluidic layer however the final cast is made thicker (~5mm) and with a 5:1 base:linker ratio. Briefly local flexure of the control layer when actuated by an external air pressure locally defines the pumps and valves which direct the flow on the bottom layer. After both the fluidic and control layers have cured, the top side of the fluidic layer and bottom side of the PDMS layer are exposed to a short air plasma treatment, aligned, placed in conformal contact and finally baked at 80^0C for two or more hours for final sealing. Figure 2 provides an overview of the fluidic fabrication procedure.

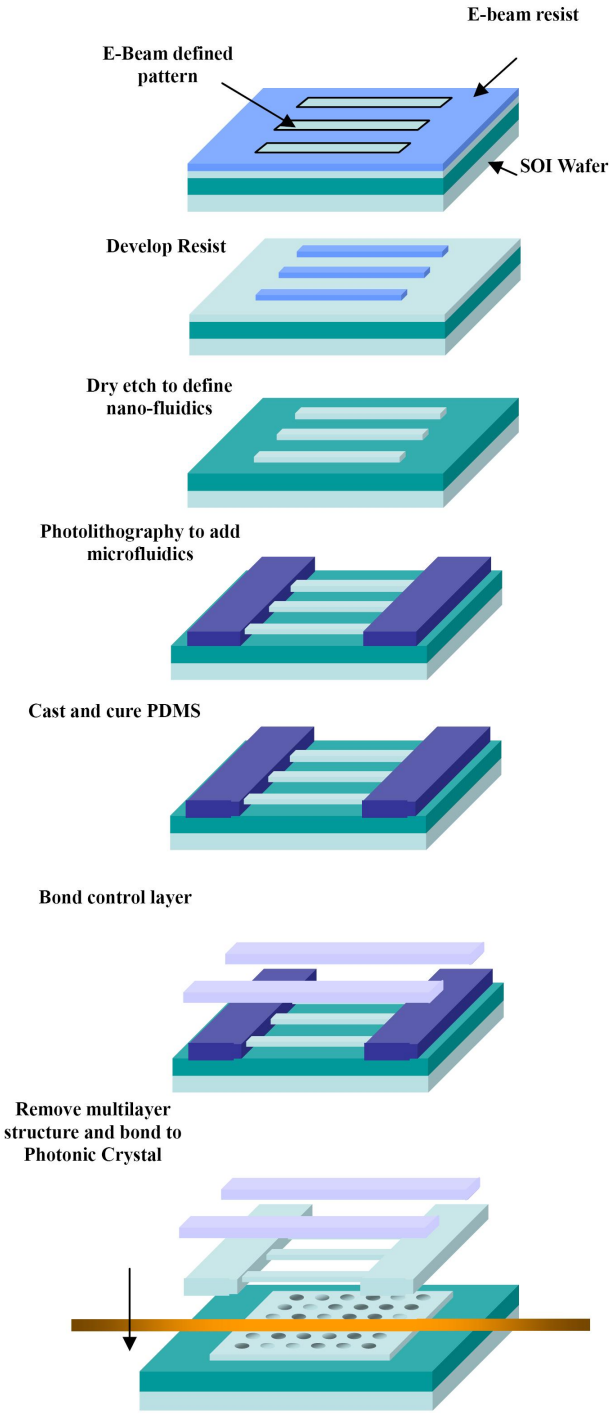

Figure 2: Overview of fabrication stages in nanoscale optofluidic integration technique.

2.4 Alignment and interfacing technique

Alignment and interfacing the sub-wavelength features in the fluidic system with the sub-wavelength features in the photonic structures, complicated by the deformable nature of the fluidic system, is one of the most challenging aspects of this work. In general parallelity between the nanochannels and the photonic structure can be achieved through standard

mechanical alignment techniques by ensuring that the alignment markers are separated by a sufficient distance. To align the system we varied the spacing between the photonic structures by one half the lattice constant, thereby ensuring alignment of at least one nanochannel (y-direction as defined in Figure 1) with the central row of at least one photonic crystal. Using this technique the two systems were positioned using a modified mask aligner and then interfaced and bonded by placing them in conformal contact after a 7s air plasma oxidation immediately prior to assembly.

As will be demonstrated in the proceeding sub-section the "zebra-spacing" technique used here was successful at aligning the nanochannels with the targeted region of the photonic structure. In general however a more precise technique for both x and y directions is required to move towards two dimensional adaptable photonic structures. At present we are investigating the use of Moiré pattern techniques[28] for performing such alignment.

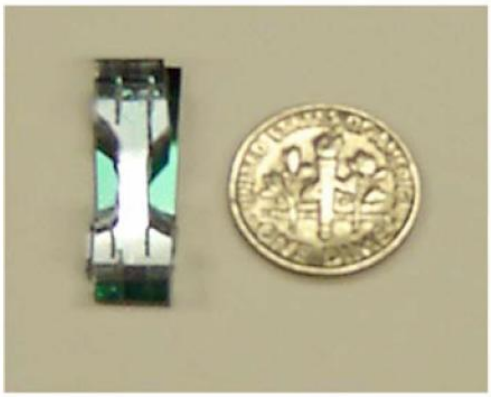

Figure 3. Photograph of an assembled chip.

2.5 Alignment, infusement and seal integrity tests

After assembly, the nanochannels were initially infused with a 1% surfactant solution of Cetyltrimethylammonium bromide (CTAB) in DI water which served to reduce the surface tension at the air liquid interface and facilitate wetting of the nanochannel arrays. As mentioned above, the air permeable nature of the RTV fluidics was also likely instrumental in removing air bubbles which may otherwise have been trapped within the system. To directly examine the channel alignment and seal integrity at the nanoscale we conducted an experiment where we initially infused a highly concentrated CTAB solution (roughly 5% by mass) into the fluidic system and allowed the solvent to evaporate overnight. Figure 3 shows an SEM image of the CTAB residue after removal of the fluidics for both an aligned and misaligned case. The seal between the elastomer and photonic crystal is quite good within the crystal itself, however there appears to be some leakage around the outside of the device where the nanochannel first comes in contact with the photonic structure and must conform to the jump interface. As can be seen however the leakage remains confined outside the device and should not significantly affect the delivery.

As can be seen in both Figure 4a and 4b the infusement into the nanowell structures appears to be complete and there does not appear to be any nano- bubbles trapped within the wells. In this case the aspect ratio of the wells (height to diameter) is 0.74. Further studies are required in order to determine what the ultimate limit on the aspect ratio is for complete wetting of the structure.

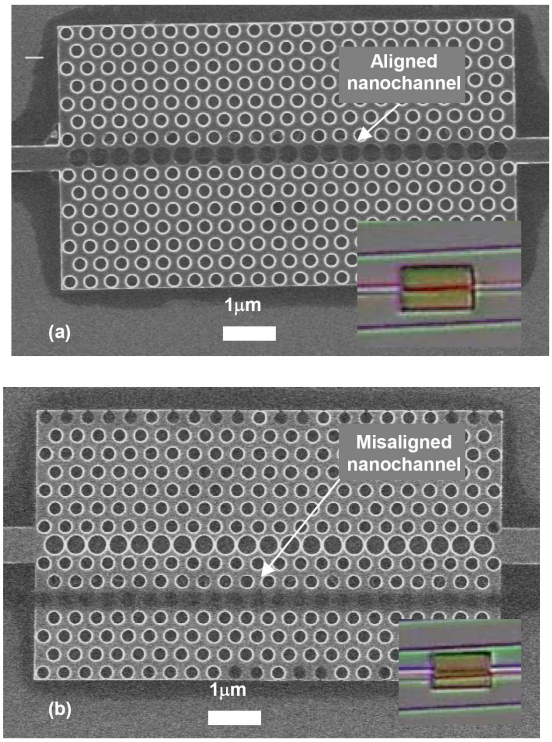

Figure 4. Demonstration of single row addressability for aligned nanochannel. (a) SEM image showing photonic crystal prior to integration with nanofluidics. Holes with increased radius define the region to be targeted fluidically. (b) SEM image of photonic crystal after removal of fluidics. Darkened regions show deposited CTAB after allowing the solvent to evaporate within the nanochannels, illustrating precise fluidic confinement within the targeted region of the photonic crystal.

3. EXPERIMENTAL SECTION

Figure 5 illustrates the experimental layout used for these experiments. A typical experiment was conducted by first adhering the optofluidic structure to the XZ chip positioning arm (as shown in 5c) and inserting the fluidic and valve tubing (as shown in 5b). The fluidic system was then wetted using the technique described above.

Liquids selected for dynamic modulation of the refractive index within the photonic structure must exhibit relatively low viscosity and high $n_{liquids}/n_{substrate}$ and must exhibit good compatibility with soft elastomers.[11] Solutions with very great ranges in refractive index are available,[29] however, the capillary pressure induced by the presence of an immiscible interface scales with 1/D and, as can be shown, at the channel scales used here this pressure becomes significantly higher than the pressure that can be applied to the system before failure of the fluidic seal. The solutions must, therefore also be miscible. As such we selected solutions of aqueous CaCl2, which ranges in composition from DI water n=1.33 to 5 M n =1.44,12 as being the most appropriate given the above requirements.

Following mounting and connection of the fluidics tapered fiber lenses (Corning, Corning NY) were mounted in the fiber alignment stages as shown and connected to the HeNe fiber laser (Thorlabs) for preliminary alignment to the on-chip waveguides. Once the preliminary alignment was done the excitation fiber was connected to the tunable infrared laser (Agilent) and the collection fiber to the power meter. The position of both stages were then optimized to maximize the transmitted power through the photonic crystal. Once the system was aligned a scan was performed with the tunable laser over the available wavelength range (1460nm to 1580nm). To determine which of the photonic crystals was aligned with the nanofluidic structure the above procedure was repeated for each photonic crystal until the expected shift in the transmission spectrum was observed (as will be demonstrated in the following section). By performing an initial diagnostic inspection of the chip using an optical microscope we were able to reduce the number of photonic crystals which may be aligned to a handful of candidates, thereby eliminating the need to scan each system to find that which

was correctly aligned.

Once the system was aligned, spectrum were taken over the range of available wavelengths for both the DI solution and 5M $CaCl_2$. Dynamic switching experiments were conducted between the two systems as will be outlined in the following section.

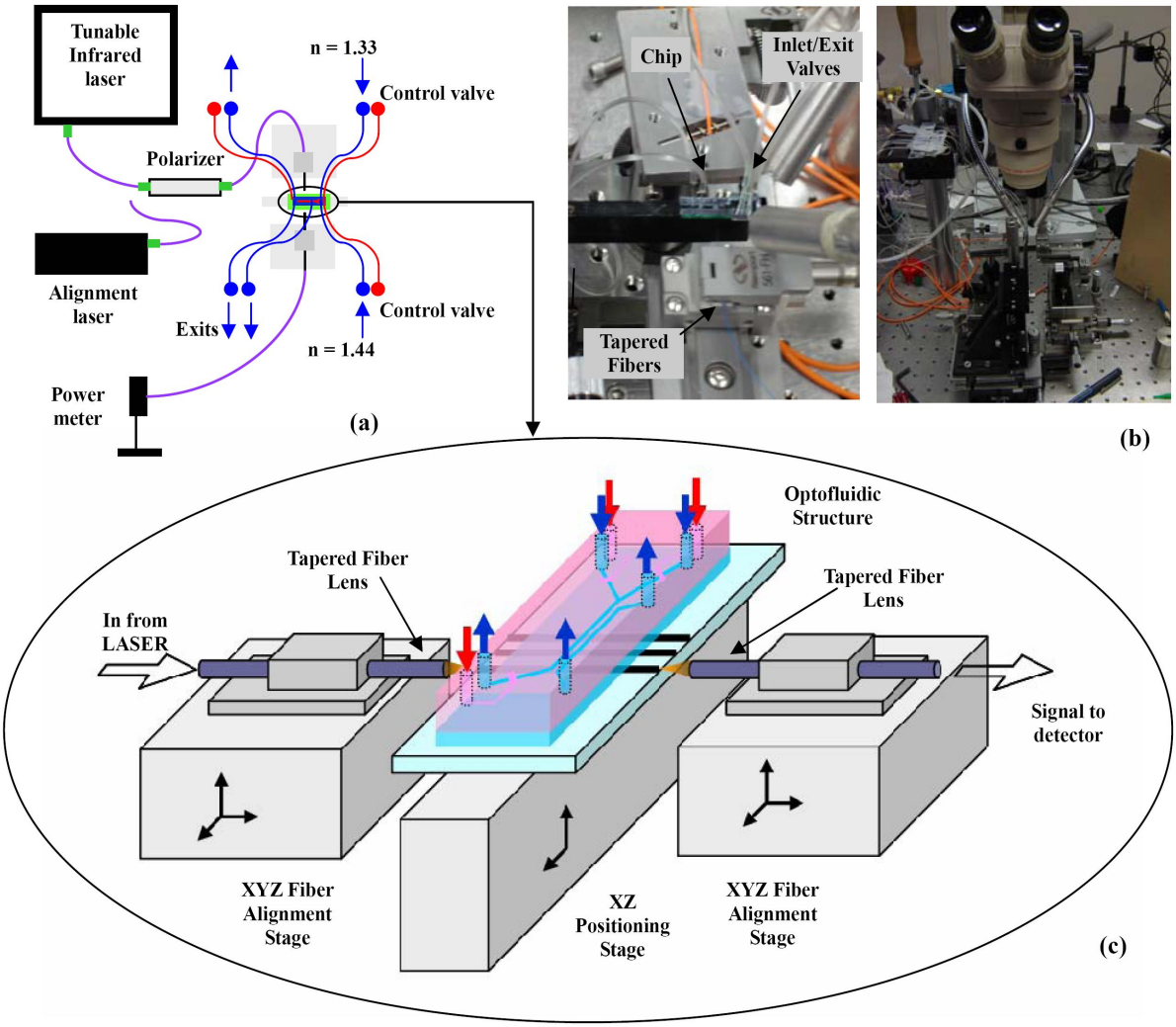

Figure 5. Nanofluidically tunable photonic crystals, experimental setup. (a) Layout of experimental setup showing fluidics, optics and positioning stages. (b) Photograph of setup (c) closeup image of the experimental apparatus.

4. NANOFLUIDIC TUNING OF PHOTONIC STRUCTURES

Figure 6a shows the normalized quasi-TE mode transmission through the photonic crystal with a fluidically modulated waveguide (i.e. central row aligned with a nanofluidic channel) for DI water and 5M $CaCl_2$. The data presented has been smoothed to remove higher frequency Fabry-Perot resonances. The results show a shift in the peak transmission of the guided mode from $a/\lambda = 0.291$ to $a/\lambda = 0.289$ (corresponding to a $\Delta\lambda$=15nm) when the lower index liquid is displaced by the higher index salt solution. The higher index solution effectively serves to decrease the size of the holes and shifts the guided mode towards the dielectric band of the regular crystal. As can be seen from Figure 6a increasing the index difference between the two fluids would provide a greater shift in the peak transmission of the guided mode, however it would not provide for a significantly higher extinction ratio. The high $\Delta n/n$ afforded by nanofluidic modulation demonstrated here enables consistently high contrast over a relatively wide range of wavelengths.

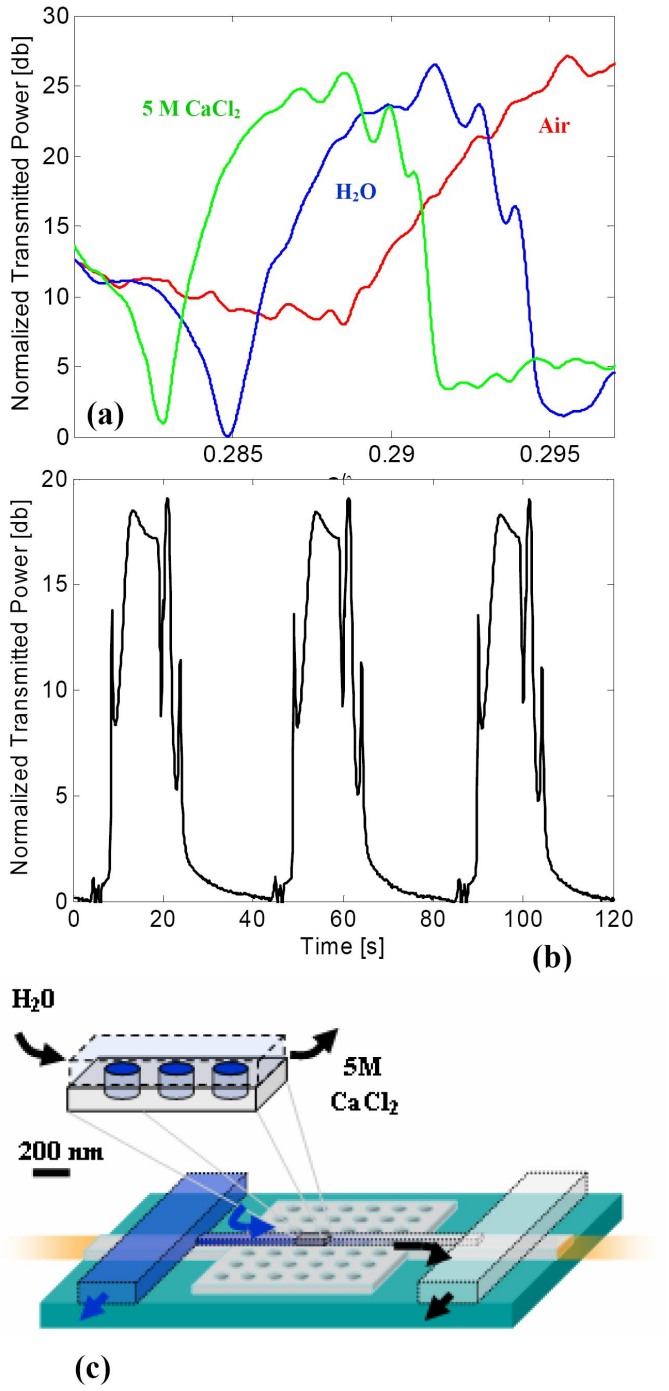

Figure 6: TE-like transmission through photonic crystal with aligned nanochannel. (a) Shift in transmitted power spectrum when aligned nanochannel filled with Air (n = 1), H20 (n = 1.33) and 5M CaCl2 (n = 1.44) (b) Dynamic switching at $a/\lambda = 0.291$. (c) Schematic showing dynamic displacement.

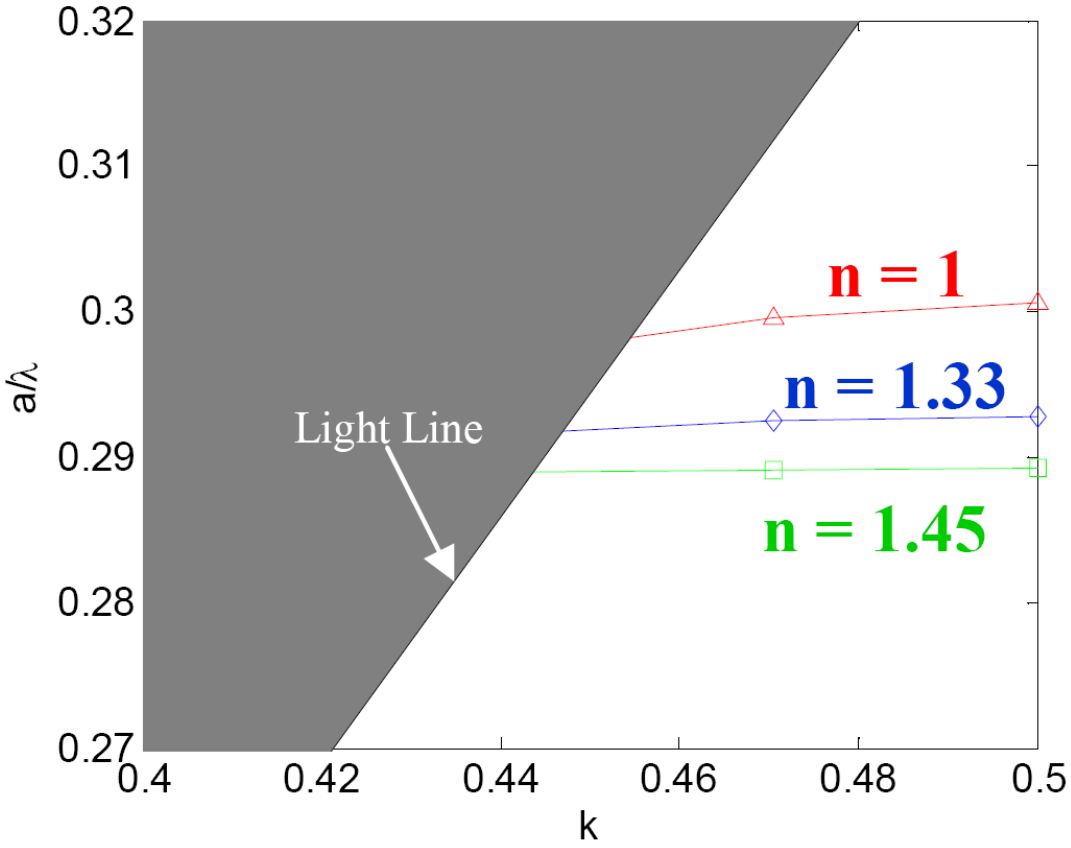

Figure 7: Dispersion diagram for TE-like modes in the for the 3D photonic crystal geometry shown in Figure 1. Lines demonstrate the change in the location of the guided mode with modulation of the refractive index in the central row of holes.

Figure 7 shows the dispersion diagram for photonic crystal geometry used here (shown in Figure 1). The n = 1 line represents the guided mode caused by the increased radius of the wholes along the center row. As the air was replaced with the higher refractive index liquids the frequency of the guided mode decreased as the optical radius of the holes became smaller. As can be seen the change the computed peak transmission wavelength matched well with that observed experimentally.

Dynamic modulation of the transmitted power is demonstrated in Figure 6b at $a/\lambda = 0.291$ by fluidically switching between the DI water and $CaCl_2$ solutions (shown schematically in Figure 6c). As can be seen extinction ratios on the order of 20dB are obtained with a switching speed on the order of 10s of seconds. The modulation speed is inherently limited by the viscous nature of the process. While accurate modeling of the fluidic transport in systems at these scales becomes exceedingly difficult (as a result of elastic deformation of the PDMS, overlapping double layers, and electroviscous effects, for example) order or magnitude estimates are possible from simple laminar flow analysis. For pressure driven flows we can estimate the timescale for hydrodynamic switching by examining the time required to completely displace one liquid with another from a nanochannel given by $t_{switch} = 12\ \eta\ L^2/\ \Delta P\ D_h^{\ 2}$. The applied pressure, ΔP, for this case was between 15 kPa and 30 kPa limited by the sealing stability between the PDMS and the photonic substrate. The channel hydraulic diameter, D_h, is fixed by the photonic geometry. The channel length, L was 400μm which could be reduced by at least an order of magnitude resulting in two order of magnitude decrease in the switching time however this is still in the millisecond range. D_h represents the most fundamental limitation on the speed of such nanoscale optofluidic devices as the geometry is fixed by the lattice constant of the photonic crystal. As an alternative

mechanism, electrokinetic transport, where flow is induced through the interaction of an applied electric field and the charge in the electrical double layer, exhibits a more favorable scaling ratio independent of D_h, $|t_s|VL^2$. Thus in principle it is more amenable to nanoscale transport and could result in lower switching times. Here, however, the low electro-osmotic mobility of the $CaCl_2$ solution made such an approach less attractive. The diffusive transport time scale into the nanowells $t_d \propto \frac{d^2}{D}$, where d is well depth and D is the diffusion coefficient) is of the order of 10^{-6} s and thus does not represent a significant limitation. The reproducible peaks in output power shown in Fig. 6b are a result of irregular bumps in the transmission spectrum of the photonic crystal as they pass through the switching wavelength. Visually, one can imagine "riding" the power curves of 6a between 0.291 and 0.289 to produce the curves of 6b.

The integration of nanofluidics with nanophotonics presents, to our knowledge, a new approach for dynamic manipulation of optical properties at subwavelength length scales. Extensions of this technique could be used to create fully reconfigurable photonic devices through arbitrary redefinition of fluidically defined defects (i.e., passive structures could be activated or defined fluidically when required and then removed later in favor of alternative functionality). Other potential functionalities include delivery of optical gain media, nonlinear liquids, or colloidal particles into arbitrary regions of these structures. Such integration could also enable a new class of resonant cavity sensors incorporating targeted delivery of single or few molecules.

ACKNOWLEDGMENTS

This work was carried out at the Center for Optofluidic Integration at the California Institute of Technology. Funding for the center is provided by the Defense Advanced Projects Agency under the University Photonics Research Centers Program.

REFERENCES

1. B. Gibson, J. R., "Liquid Mirror Telescopes – History,"Astron. Soc. Can. 85, 158 (1991).
2. S. Kuiper and B. Hendriks, "Variable-focus liquid lens for miniature cameras,"Appl. Phys. Lett. 85, 1128 (2004).
3. D. Wolfe, R. Conroy, P. Garstecki, B. Mayers, M. Fischback, K. Paul, M. Prentiss, and G. Whitesides, "Development of a fret biosensor to detect the pathogen *mycoplasma capricolum*,"Proc. Natl. Acad. Sci. U.S.A. 101, 12434 (2004).
4. P. Mach, M. Dolinski, K. Baldwin, J. Rogers, C. Kerbage, R. Windeler, and B. Eggleton, "Tunable microfluidic optical fiber," Appl. Phys. Lett. 80, 4294 (2002).
5. P. Domachuck, H. C. Nguyen, B. J. Eggleton, M. Straub, and M. Gu, "Microfluidic tunable photonic band-gap device," Appl. Phys. Lett. 84, 1838 (2004).
6. B. Maune, M. Loncar, J. Witzens, M. Hochberg, T. Baehr-Jones, D. Psaltis, A. Scherer, and Y. Qiu, "Liquid-crystal electric tuning of a photonic crystal laser," Appl. Phys. Lett. 85, 360 (2004).
7. V. Almeida, C. Barrios, R. Panepucci, and M. Lipson, "All-optical control of light on a silicon chip," Nature 431, 1081 (2004)
8. M. Unger, H. Chou, T. Thorsen, A. Scherer, and S. Quake, "Monolithic Microfabricated Valves and Pumps by Multilayer Soft Lithography," Science 288, 113 (2000)
9. J. Joannopoulos, R. Meade, and J. Winn, *Photonic Crystals: Molding the Flow of Light* (Princeton U. Press, 1995).
10. M. Loncar, D. Nedeljkovic, T. Doll, J. Vuckovic, A. Scherer, and T. Pearsall, "Waveguiding in planar photonic crystals ,"Appl. Phys. Lett. 77, 1937 (2000).
11. J. Lee, C. Park, and G. Whitesides, "PDMS absorption of small molecules and consequences in microfluidic applications,"Anal. Chem. 75, 6544 (2003).
12. D. Lide, ed., *Handbook of Chemistry and Physics*, 79th ed. (CRC Press, 1999).
13. Loncar, M., Nedeljkovic, D., Doll, T., Vuckovic, J., Scherer, A., Pearsall, T., 2000, "Waveguiding in Planar Photonic Crystals" App Phys Lett. 77 1937.
14. Manz, A., Graber, N., Widmer, H., 1990, "Miniaturized total chemical analysis systems – A novel concept for chemical sensing" Sens. Actuators B 1 244.
15. Manz, A., Harrison, D., Verpoorte, E., Fettinger, J., Paulus, A., Ludi, H., Widmer, H., 1992, "Planar chips technology for miniaturization and integration of separation techniques into monitoring systems – capillary electrophoresis on a chip" J. Chromatography, 593 253.
16. Harrison, D., Fluri, K., Seiler, K., Fan, Z., Effenhauser, C.,Manz, A., 1993a, "Micromachining a miniaturized

capillary electrophoresis-based chemical-analysis systems on a chip" Science 261, 895.
17. Petersen, K., 1982, "Silicon as a mechanical material" Proceedings of the IEEE 70 420.
18. Wise, K., Najafi, K., 1991, "Microfabrication techniques for integrated sensors and microsystems" Science 254, 1335.
19. Chabinyc, M., Chiu, D., McDonald, J., Stroock, A., Christian, J., Karger, A., Whitesides, G., 2001, "An integrated fluorescence detection system in poly(dimethylsiloxane) for microfluidic applications" Anal. Chem. 73 4491.
20. Duffy, D., McDonald, J., Schueller, O., Whitesides, G., 1998 "Rapid prototyping of microfluidic systems in poly(dimethylsiloxane)" Anal. Chem. 70, 4974.
21. Johnson, R, Badr,, I., Barrett, G., Lai, S., Lu, Y., Madou, M., Bachas, L., 2001, "Development of a fully integrated analysis system for ions based on ion-selective optodes and centrifugal microfluidics" Anal. Chem. 73, 3940.
22. Pugmire, D., Waddell, E., Haasch, R., Tarlov, M.,
Locascio, L., 2002, "Surface characterization of laserablated polymers used for microfluidics" Anal. Chem. 74, 871.
23. Becker H., Locascio, L.E., 2002, "Polymer microfluidic devices" Talanta, 56, 267.
24. deMello, A., 2002, "Microfluidics - DNA amplification
moves on" Lab Chip, 2, 31N-36N.
25. Schueller, O., Brittain, S., Whitesides, G., 1999, "Fabrication of glassy carbon microstructures by soft lithography" Sensors and Actuators A, 72 125.
26. Schueller, O., Duffy, D., Rogers, J., Brittain, S., Whitesides, G., 1998, "Reconfigurable diffraction gratings based on elastomeric microfluidic devices" Sensors Actuators A, 78, 149.
27. Thorsen, T., Maerkl, S., Quake, S., 2002, "Microfluidic
large-scale integration" Science 298 580.
28. King, M., Berry, D., 1972 "Photolithographic Mask Alignment using Moire Techniques" App. Optics, 11 2455.
29. Erickson, D., Heng, X., Li, Z., Rockwood, T., Emery, T.,Zhang, Z., Scherer, A., Yang, C., Psaltis, D., "Optofluidics" SPIE Optics and Photonics Meeting, August 2005, San Diego.